

Self-Equilibration of the Diameter of Ga-Catalyzed GaAs Nanowires

V. G. Dubrovskii,^{†,‡,§} T. Xu,^{||,⊥} A. Díaz Álvarez,^{||} S. R. Plissard,^{||,#} P. Caroff,^{||,▽} F. Glas,[○] and B. Grandidier^{*,||}

[†]St. Petersburg Academic University, Khlopina 8/3, 194021, St. Petersburg, Russia

[‡]Toffe Physical Technical Institute RAS, Politekhnikeskaya 26, 194021, St. Petersburg, Russia

[§]ITMO University, Kronverkskiy pr. 49, 197101 St. Petersburg, Russia

^{||}Institut d'Electronique, de Microélectronique et de Nanotechnologies (IEMN), CNRS, UMR 8520, Département ISEN, 41 bd Vauban, 59046 Lille Cedex, France

[⊥]Sino-European School of Technology, Shanghai University, 99 Shangda Road, Shanghai, 200444, People's Republic of China

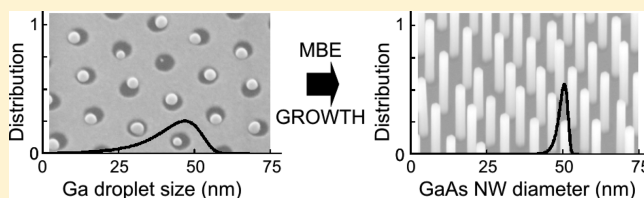
[#]CNRS-Laboratoire d'Analyse et d'Architecture des Systèmes (LAAS), Université de Toulouse, 7 avenue du colonel Roche, 31400 Toulouse, France

[▽]Department of Electronic Materials Engineering, Research School of Physics and Engineering, The Australian National University, Canberra, ACT 0200, Australia

[○]CNRS-Laboratoire de Photonique et de Nanostructures (LPN), Route de Nozay, 91460 Marcoussis, France

ABSTRACT: Designing strategies to reach monodispersity in fabrication of semiconductor nanowire ensembles is essential for numerous applications. When Ga-catalyzed GaAs nanowire arrays are grown by molecular beam epitaxy with help of droplet-engineering, we observe a significant narrowing of the diameter distribution of the final nanowire array with respect to the size distribution of the initial Ga droplets. Considering that the droplet serves as a nonequilibrium reservoir of a group III metal, we develop a model that demonstrates a self-equilibration effect on the droplet size in self-catalyzed III–V nanowires. This effect leads to arrays of nanowires with a high degree of uniformity regardless of the initial conditions, while the stationary diameter can be further finely tuned by varying the spacing of the array pitch on patterned Si substrates.

KEYWORDS: III–V nanowires, silicon integration, self-catalyzed growth, growth kinetics, size distribution, focusing effect



Growing semiconductor materials with high precision at the nanoscale is essential to improve the efficiencies of ongoing technologies.^{1–4} Among the existing growth methods for compound semiconductor nanostructures, a few rely on the use of a tiny reservoir consisting of one of the elements composing the nanostructure. A prototypical case is a reservoir of the group III metal during growth of III–V compound semiconductors. Such a reservoir initiates or fuels epitaxial growth leading to the formation of nanostructures with specific geometries such as rings and wires.^{5–7} For nanowires (NWs), the so-called self-catalyzed growth is based on the vapor–liquid–solid (VLS) mechanism assisted by a group III metal droplet and has been successfully demonstrated with Ga droplets and also In droplets.^{8–13} In contrast to the other common Si-compatible growth technique, namely the catalyst-free selective-area epitaxy,^{14,15} self-seeded NWs have been shown to easily reach crystal phase purity.^{9,16,17}

In the self-catalyzed VLS growth, the NW elongation rate is controlled entirely by the kinetics of group V species,^{6,18} while the catalyst particle undergoes a significant and unavoidable attachment and detachment of group III metal atoms. The incoming atoms can either directly impinge from vapor or diffuse from the NW sidewalls to feed the droplet. Changing

the different fluxes can thus result in a significant modification of the NW morphology including the NW diameter, because the latter is known to be governed by the size of the droplet.^{18–20} As homogeneity of the NW diameter and shape is essential for making reproducible devices^{21,22} and crucial for improving the collective properties of NW arrays,^{23,24} there is a strong demand to control the behavior of the droplet size in the self-catalyzed VLS growth.

Here, we examine the diameter evolution of Ga-catalyzed GaAs NWs grown by droplet-engineered molecular beam epitaxy (MBE). Such a method has been shown to give a high yield of vertical GaAs NWs when a Ga predeposition step is added prior to growth initiation and when a good control over the surface properties of the patterned material exposed to growth is achieved.^{25–27} As a new milestone, we show that under appropriate growth conditions the NW diameters converge toward a critical value that is directly related to the size evolution of the droplet during the self-catalyzed growth. By theoretically investigating the dynamical change of the

Received: June 5, 2015

Revised: June 29, 2015

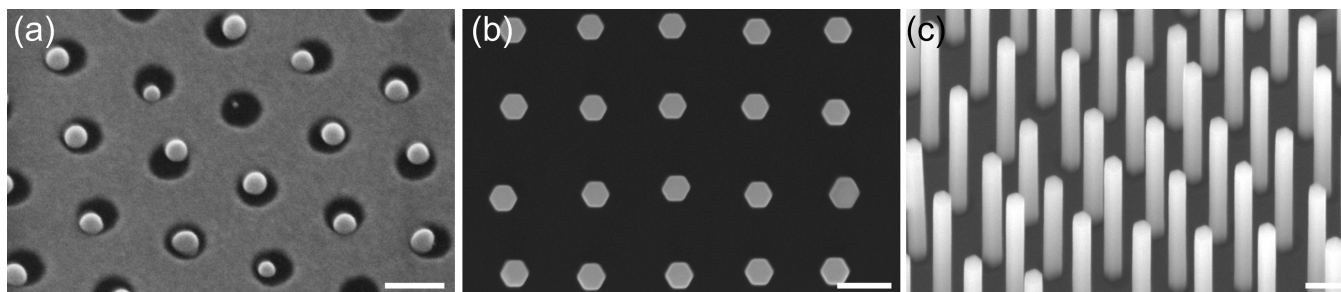


Figure 1. (a) A 30° tilted SEM image of Ga droplets obtained after predeposition of Ga onto a hole array defined in a SiO₂ native oxide on a Si(111) substrate using electron beam lithography and etching. The diameter of the holes is 60 nm and the pitch between the holes is 100 nm. (b,c) Top view and 30° tilted SEM images of self-catalyzed GaAs NWs grown from the array of Ga droplets shown in (a). The scale bar corresponds to 100 nm.

droplet size as a function of the incoming flux and the crystallization rate of the NW, we demonstrate the key role of the diffusion-induced contribution of Ga adatoms in focusing the droplet size distribution. This self-equilibration of the droplet size in self-catalyzed III–V NWs enables the formation of unique NW arrays with very narrow distribution of the NW diameters despite being initially grown from differently sized droplets. The critical diameter can be further finely tuned by the wire-to-wire spacing.

In our experiments, the growth of GaAs NW on Si(111) substrates was achieved through three steps, as described previously:²⁸ (i) patterning of a hole array in a thin silicon dioxide layer to allow the precise positioning of the NWs on a silicon substrate, (ii) predeposition of Ga to form droplets in the etched holes and (iii) MBE growth of NWs. The NW growth was performed at a temperature of 630 °C, an As/Ga growth rate equivalent ratio of 1.8 and a two-dimensional equivalent growth rate of GaAs of one monolayer per second. Figure 1 shows scanning electron microscopy (SEM) images obtained after steps (ii) and (iii) for an array of holes with a diameter of 60 nm and a pitch of 100 nm. It is seen that the Ga predeposition leads to the formation of Ga droplets in the oxide-free openings only, resulting in the growth of NWs at the position of the holes. While the diameter of the Ga droplets varies significantly from hole to hole (the droplet diameter distribution may depend on the droplet preparation process but is never uniform), we notice a high degree of uniformity of the NW diameters with minimal tapering effect due to the low V/III ratio.

This difference between the droplet size distribution and the NW diameter distribution was reproducible, whatever the initial size and the pitch between the holes in the array were. For example, Figure 2 compares the size distribution of the Ga droplets with the distribution of the NW diameters for an array with a hole size of 60 nm and a pitch of 250 nm. Again, the NWs in the array are quite uniform and the NW diameter distribution appears clearly much narrower than the hole size distribution. Remarkably, the Ga-catalyzed growth of NWs leads to a focusing effect toward a diameter of ~50 nm, slightly bigger than the peak value of the droplet size distribution, but still smaller than the hole size. In order to understand this striking difference, we establish the following model.

As mentioned above, the elongation rate of Ga-catalyzed GaAs NWs is limited by the kinetics of As species that arrive at and desorb from the droplet surface but do not diffuse from the sidewalls.^{6,18,29,30} Because of a known low solubility of As in liquid Ga, the catalyst droplet consists of almost pure Ga and serves as a Ga reservoir for arriving As species. Therefore, the

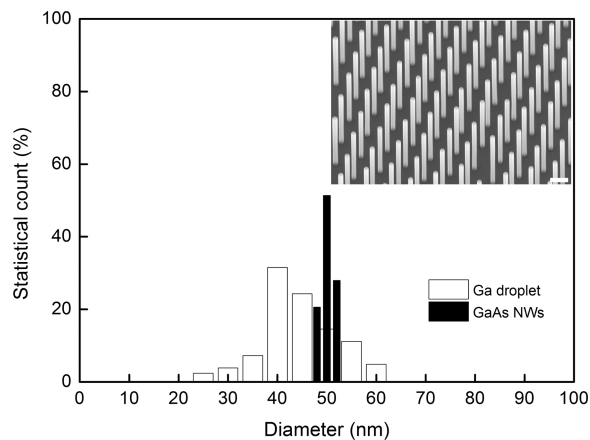


Figure 2. Histograms of the Ga droplet size distribution and the NW diameter distribution. Inset: 30° tilted SEM images of the corresponding array of GaAs NWs. For this array, the hole size and pitch are 60 and 250 nm, respectively. Scale bar in the inset corresponds to 100 nm.

droplet can either inflate or shrink with time depending on the balance of Ga species.¹⁸ Indeed, the total number of Ga atoms in the droplet N changes in time according to

$$\frac{dN}{dt} = \chi I \pi R^2 + 2l\lambda R \sin \alpha - \frac{\pi R^2}{\Omega_{\text{GaAs}}} \frac{dL}{dt} \quad (1)$$

Here, I is the direct atomic flux of Ga, χ is the geometrical function that depends on the contact angle β of the droplet and the incident angle α of the Ga beam and equals $1/\sin^2 \beta$ when $\beta \geq \pi/2 + \alpha$,³¹ R is the radius of cylindrical NW, λ is the effective diffusion length of Ga adatoms on the NW sidewalls, $\Omega_{\text{GaAs}} = 0.0452 \text{ nm}^3$ is the volume per GaAs pair in the solid and dL/dt is the NW elongation rate. The first term stands for the direct impingement of Ga, the second gives the diffusion-induced contribution of Ga adatoms from the length λ beneath the droplet (more complex scenarios of the diffusion fluxes are given, for example, in refs 32 and 33) and the third describes the sink due to the NW elongation.

The droplet volume equals $V = \Omega_{\text{Ga}} N = (\pi R^3/3)f(\beta)$, where $\Omega_{\text{Ga}} = 0.02 \text{ nm}^3$ is the Ga atomic volume in liquid³⁴ and $f(\beta) = (1 - \cos \beta)(2 + \cos \beta)/[(1 + \cos \beta)\sin \beta]$ is the geometrical function relating the volume of a spherical cap to the radius of its base. Assuming β as being independent of radius and using eq 1, we arrive at

$$\frac{dR}{dt} = -A + \frac{B}{R} \quad (2)$$

with

$$A = \frac{\Omega_{\text{Ga}}}{\Omega_{\text{GaAs}} f(\beta)} \left(\frac{dL}{dt} - \chi\nu \right); \quad B = \frac{2\Omega_{\text{Ga}}}{\pi\Omega_{\text{GaAs}} f(\beta)} \nu\lambda \sin\alpha \quad (3)$$

and $\nu = \Omega_{\text{GaAs}}$ as the Ga deposition rate in nm/s. Obviously, the behavior of the NW radius is very different at $A > 0$ and $A < 0$. When the effective Ga imbalance is positive ($A < 0$), that is, more Ga atoms are brought from vapor to the droplet than removed from it to grow a NW, the droplet will inflate with the help of surface diffusion (B) and consequently the NW will extend radially regardless of its initial dimension (the regime of radial growth).¹⁸ This situation corresponds to low As influx which yields small elongation rates such that $dL/dt < \chi\nu$. Whenever $A > 0$, that is, more Ga atoms are removed from the droplet due to crystallization than brought from vapor, the situation becomes completely different. An additional diffusion flux of sidewall Ga adatoms will have a focusing effect on the diameter, that is, small NWs with $R < R_c$ will extend and large NWs with $R > R_c$ shrink to reach the critical radius $R_c = B/A$ (the regime of diameter self-equilibration).

The radius distribution $f(R, t)$ of NWs at time t obeys the following first order equation^{35,36}

$$\frac{\partial f(R, t)}{\partial t} = -\frac{\partial}{\partial R} \left[\frac{dR}{dt} f(R, t) \right] \quad (4)$$

where the initial condition is determined by the size distribution of Ga droplets prior to growth. Introducing the scaled size $r = R/R_c$ and scaled time $x = t/\tau$ with $\tau = R_c/A = B/A^2$ as the characteristic relaxation time, solutions to eqs 2 and 4 can be put in the universal form with the minimized number of parameters. The time-dependent radius of individual NW that has emerged from the droplet of radius $r_0 = R_0/R_c$ at $t = 0$ is given by

$$x = r_0 - r + \ln \left(\frac{r_0 - 1}{r - 1} \right) \quad (5)$$

In particular, this equation applies to the most representative NW radius $r_*(x)$ which corresponds to the most representative size of the initial droplets r_*^0 at $t = 0$. The size distribution is obtained in the form:

$$f(r, x) = \frac{cr}{|r-1|} g \left[r_*(x) - r + \ln \left| \frac{r_*(x) - 1}{r - 1} \right| \right] \quad (6)$$

where the time dependence $r_*(x)$ is determined by eq 5 with $r_0 = r_*^0$. The shape of the function $g(y)$ is time-invariant and is defined by the initial size distribution of the Ga droplets, while the time evolution of the NW diameter distribution is described by the time dependence of the most representative size $r_*(x)$. The combination of variables in the argument of g is the first integral of eq 4, while the prefactor c ensures the correct normalization of the distribution.

Figure 3 shows the narrowing effect in the scaled variables for an ensemble of droplets described by the Gaussian distribution $g(y) = (1/\Delta r\sqrt{\pi}) \exp(-y^2/\Delta r^2)$ with the initial distribution width $\Delta r = 0.5$ and the initial mean size $r_*^0 = 1.5$. It is seen that our nonlinear system features quite unique behavior where the mean size self-equilibrates to R_c and this process gradually decreases the effective width of the size distribution.

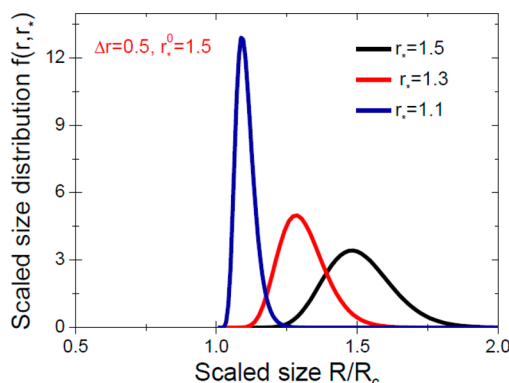


Figure 3. Evolution of the initial radius distribution with the width $\Delta r = 0.5$ to a much narrower distribution as the scaled mean size tends to one.

To observe this focusing effect on the diameters of Ga-catalyzed NWs, one needs to fulfill the condition $dL/dt > \chi\nu$, which requires high enough As influx. In our case, the GaAs NWs reach $\sim 1 \mu\text{m}$ length after 300 s of growth, therefore the average elongation rate equals $dL/dt = 3.33 \text{ nm/s}$. The equivalent two-dimensional growth rate $\nu \cos\alpha$ equals 0.326 nm/s , yielding $\nu = 0.360 \text{ nm/s}$ at $\alpha = 25^\circ$. Taking the average value of the contact angle $\beta = 115^\circ$, we obtain the Ga flux impinging the droplet at $\chi\nu = 0.438 \text{ nm/s}$. Therefore, the difference $dL/dt - \chi\nu = 2.89 \text{ nm/s}$ in our case is positive and large, which definitely favors the self-equilibration regime. With these plausible parameters, we obtain $A = 0.300 \text{ nm/s}$. Using the value of R_c of 25 nm (because the critical diameter is close to 50 nm from Figure 2), we arrive at $B = 7.50 \text{ nm}^2/\text{s}$. On the basis of eq 3, we deduce a reasonable estimate for the effective diffusion length of Ga adatoms at the NW sidewalls of $\lambda = 750 \text{ nm}$. Indeed, with the effective distance between the neighboring NWs of approximately 250 nm the collection length limited by the shadow effect in this array^{37,38} would be about 540 nm. Larger λ obtained from our fits should be due to the simplified form of the Ga diffusion flux in eq 1 that does not precisely describe the initial growth stage at $L < \lambda$.^{31,32} Finally, the relaxation time τ equals 83 s, which is noticeably shorter than the total growth time of 300 s. The distribution of the NW top diameters is therefore expected to be almost completely equilibrated after stopping the growth.

Figure 4 shows the plots of NW diameters $D = 2R$ versus time obtained from eq 5 with the above parameters and at different initial droplet diameters ranging from 25 to 60 nm. The effect of self-equilibration is clearly seen and correlates with the experimental histograms at $t_g = 300 \text{ s}$. The size distribution is narrowed from 25 to 60 nm to $\sim 50 \text{ nm}$, as observed in Figure 2, while thinner and thicker NWs are no longer present in the histograms. The described effect is very important because it will transform an arbitrary broad diameter distribution of the initial Ga droplets to the asymptotically uniform distribution provided that the growth time is long enough to allow for the complete size relaxation. After reaching this size-uniform state, the NWs will continue to elongate with stationary diameter and at almost diameter-independent rate that also yields the uniform length. This explains why the ensembles of Ga-catalyzed GaAs NWs usually have more uniform dimensions compared to Au-catalyzed ones.³⁹

According to the quantitative nucleation-based model of Glas et al.,³⁰ the growth rate of a self-catalyzed NW under steady

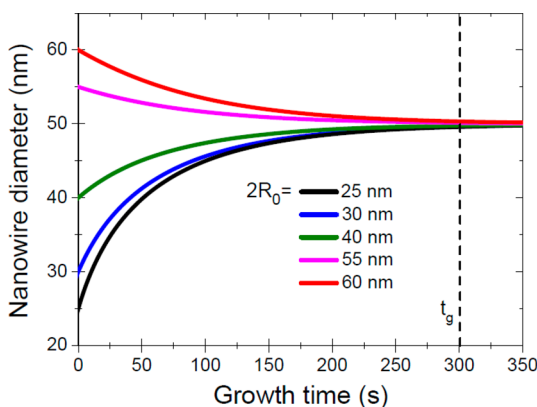


Figure 4. Theoretical time-dependent variations of the NW diameters obtained from eq 5 with different R_0 . The vertical dash segment indicates the experimental growth time t_g of 300 s.

state fluxes depends on the NW radius (this is partly due to the different areas available for nucleation at the liquid–solid interface of differently sized NWs). The fact that narrow NWs may grow very slowly should effectively produce some reduction of NW radius distribution with respect to an initial droplet diameter distribution. However, the same does not hold for large NW radii and the expected narrowing is much less marked than in the present model. Moreover, the analysis of ref 30, assumes a constant radius for each NW and therefore ignores the self-equilibration mediated by radius changes that is described here. In this sense, the diameter self-equilibration in self-catalyzed III–V NWs resembles the height equilibration of self-induced GaN NWs.⁴⁰ This effect is caused by completely different physical reasons but also leads to stable asymptotic size-uniformity, while narrowing the length distribution of Ge NWs described in ref 33 could be reached only at a certain moment of time. We also note that a diameter self-regulation in array of NWs has recently been reported for catalyst-free, spontaneously formed GaN NWs.⁴¹ However, the mechanism of the diameter self-equilibration in our case is different and is associated with the reservoir effect of nonequilibrium Ga droplet while no such droplet is present on top of any self-induced NWs.

Furthermore, Figure 5 shows that the stationary diameter of NWs can be tuned by the pitch of the Ga droplet array. The normalized histograms of the diameter distributions show the large dispersion of the Ga droplet sizes that equilibrate to regular arrays of 50, 60, and 70 nm diameter NWs in the course of growth for the pitch of 250, 500, and 1000 nm, respectively. The diameter distributions are fitted by eqs 5 and 6 with the same parameter as before but with different $2R_c \sim 50, 60,$ and 70 nm depending on the pitch. The increase of the stationary diameter is well-understood through the shadowing effect,^{37,38} which is important for the smallest pitch but vanishes for the large pitches. Thus, the effective collection length of Ga increases for larger pitches and finally becomes limited by the Ga incorporation to the growing shells around the NW (this process is necessary to maintain a uniform NW diameter from base to top). The increase of λ raises the B value in eq 3 and therefore results in the larger stationary diameter that is proportional to B . In other words, the Ga transport into the droplet can be regulated by the wire-to-wire spacing and the resulting NW diameter can be finely tuned to the desired value.

In conclusion, we have demonstrated experimentally and described theoretically the effect of the diameter self-

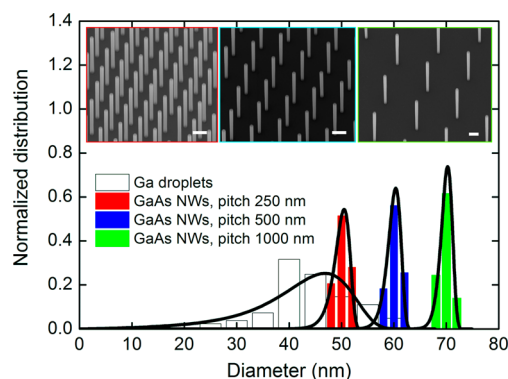


Figure 5. Histograms showing the distribution of the Ga droplet size and NW diameter for arrays with a hole size of 60 nm and three different pitches (left, 250 nm; middle: 500 nm; right, 1000 nm). Inset: 30° tilted SEM images of the corresponding GaAs NW arrays. The scale bar is 200 nm. The solid lines show the theoretical fits obtained from eqs 5 and 6.

equilibration in Ga-catalyzed GaAs NWs that produces regular arrays of NWs regardless of the initial droplet size distribution. This effect is not at all restricted to particular epitaxy technique or deposition conditions and should be observed in all self-catalyzed VLS systems where the low vapor flux of a group III metal is compensated by diffusion of surface adatoms. The resulting NW arrays show a very high degree of the diameter uniformity while the stationary diameter can be tuned by the growth conditions or geometrical parameters such as the array pitch on patterned Si substrates. The described self-equilibration effect is important from the fundamental viewpoint and should be useful for applications that require the controlled fabrication of regular NW arrays with tunable diameters.

AUTHOR INFORMATION

Corresponding Author

*E-mail: bruno.grandidier@isen.iemn.univ-lille1.fr.

Notes

The authors declare no competing financial interest.

ACKNOWLEDGMENTS

This study was supported by the European Community's Seventh Framework Program (Grant PITN-GA-2012-316751, "Nanoembrace" Project), the EQUIPEX program Excelsior, the RENATECH network. T.X. acknowledges the supports of the Region Nord-Pas-de-Calais and of the National Natural Science Foundation of China (Grant 61204014). V.G.D. thanks the Russian Science Foundation for the financial support received under the Grant 14-22-00018.

REFERENCES

- (1) Tian, B.; Zheng, X.; Kempa, T. J.; Fang, Y.; Yu, N.; Yu, G.; Huang, J.; Lieber, C. M. *Nature* **2007**, *449*, 885–890.
- (2) Dousse, A.; Suffczynski, J.; Beveratos, A.; Krebs, O.; Lemaître, A.; Sagnes, I.; Bloch, J.; Voisin, P.; Senellart, P. *Nature* **2010**, *466*, 217–220.
- (3) Bulgarini, G.; Reimer, M. E.; Hocevar, M.; Bakkers, E. P. A. M.; Kouwenhoven, L. P.; Zwiller, V. *Nat. Photonics* **2012**, *6*, 455–458.
- (4) Schneider, C.; et al. *Nature* **2013**, *497*, 348–352.
- (5) Mano, T.; Kuroda, T.; Sanguinetti, S.; Ochiai, T.; Tateno, T.; Kim, J.; Noda, T.; Kawabe, M.; Sakoda, K.; Kido, G.; Koguchi, N. *Nano Lett.* **2005**, *5*, 425–428.

- (6) Colombo, C.; Spirkoska, D.; Frimmer, M.; Abstreiter, G.; Fontcuberta i Morral, A. *Phys. Rev. B: Condens. Matter Mater. Phys.* **2008**, *77*, 155326.
- (7) Zhou, Z. Y.; Zheng, C. X.; Tang, W. X.; Tersoff, J.; Jesson, D. E. *Phys. Rev. Lett.* **2013**, *111*, 036102.
- (8) Jabeen, F.; Grillo, V.; Rubini, S.; Martelli, F. *Nanotechnology* **2008**, *19*, 275711.
- (9) Krogstrup, P.; Popovitz-Biro, R.; Johnson, E.; Madsen, M. H.; Nygård, J.; Shtrikman, H. *Nano Lett.* **2010**, *10*, 4475–4482.
- (10) Plissard, S.; Dick, K. A.; Larrieu, G.; Godey, S.; Addad, A.; Wallart, X.; Caroff, P. *Nanotechnology* **2010**, *21*, 385602.
- (11) Dimakis, E.; Lähmann, J.; Jahn, U.; Breuer, S.; Hulse, M.; Geelhaar, L.; Riechert, H. *Cryst. Growth Des.* **2011**, *11*, 4001–4008.
- (12) Grap, T.; Rieger, T.; Blömers, C.; Schäpers, T.; Grützmacher, D.; Lepsa, M. I. *Nanotechnology* **2013**, *24*, 335601.
- (13) Biermanns, A.; Dimakis, E.; Davydok, A.; Sasaki, T.; Geelhaar, L.; Takahashi, M.; Pietsch, U. *Nano Lett.* **2014**, *14*, 6878–6883.
- (14) Tomioka, K.; Kobayashi, Y.; Motohisa, J.; Hara, S.; Fukui, T. *Nanotechnology* **2009**, *20*, 145302.
- (15) Björk, M. T.; Schmid, H.; Breslin, C. M.; Gignac, L.; Riel, H. J. *Cryst. Growth* **2012**, *344*, 31–37.
- (16) Cirlin, G. E.; Dubrovskii, V. G.; Samsonenko, Y. B.; Bouravleuv, A. D.; Durose, K.; Proskuryakov, Y. Y.; Mendes, B.; Bowen, L.; Kaliteevski, M. A.; Abram, R. A.; Zeze, D. *Phys. Rev. B: Condens. Matter Mater. Phys.* **2010**, *82*, 035302.
- (17) Conesa-Boj, S.; Kriegner, D.; Han, X.-L.; Plissard, S.; Wallart, X.; Stangl, J.; Fontcuberta i Morral, A.; Caroff, P. *Nano Lett.* **2014**, *14*, 326–332.
- (18) Priante, G.; Ambrosini, S.; Dubrovskii, V. G.; Franciosi, A.; Rubini, S. *Cryst. Growth Des.* **2013**, *13*, 3976–3984.
- (19) Cui, Y.; Lauhon, L. J.; Gudixsen, M. S.; Wang, J.; Lieber, C. M. *Appl. Phys. Lett.* **2001**, *78*, 2214–2216.
- (20) Somaschini, C.; Bietti, S.; Trampert, A.; Jahn, U.; Hauswald, C.; Riechert, H.; Sanguinetti, S.; Geelhaar, L. *Nano Lett.* **2013**, *13*, 3607–3613.
- (21) Fan, Z.; Ho, J. C.; Jacobson, Z. A.; Razavi, H.; Javey, A. *Proc. Natl. Acad. Sci. U. S. A.* **2008**, *105*, 11066–11070.
- (22) Tomioka, K.; Yoshimura, M.; Fukui, T. *Nature* **2012**, *488*, 189–192.
- (23) Wang, Z. K.; Lim, H. S.; Zhang, V. L.; Goh, J. L.; Ng, S. C.; Kuok, M. H.; Su, H. L.; Tang, S. L. *Nano Lett.* **2006**, *6*, 1083–1086.
- (24) Kelzenberg, M. D.; Boettcher, S. W.; Petykiewicz, J. A.; Turner-Evans, D. B.; Putnam, M. C.; Warren, E. L.; Spurgeon, J. M.; Briggs, R. M.; Lewis, N.; Atwater, H. A. *Nat. Mater.* **2010**, *9*, 239–244.
- (25) Russo-Averchi, E.; Vukajlovic Plestina, J.; Tütüncüoğlu, G.; Matteini, F.; Dalmau Mallorqui, A.; de la Mata, M.; Rüffer, D.; Potts, H. A.; Arbiol, J.; Conesa-Boj, S.; Fontcuberta i Morral, A. *Nano Lett.* **2015**, *15*, 2869–2874.
- (26) Matteini, F.; Tütüncüoğlu, G.; Potts, H. A.; Jabeen, F.; Fontcuberta i Morral, A. *Cryst. Growth Des.* **2015**, *15*, 3105.
- (27) Munshi, A. M.; Dheeraj, D. L.; Fauske, V. T.; Kim, D. C.; Huh, J.; Reinertsen, J. F.; Ahtapodov, L.; Lee, K. D.; Heidari, B.; van Helvoort, A. T.; Fimland, B. O.; Weman, H. *Nano Lett.* **2014**, *14*, 960–966.
- (28) Plissard, S.; Larrieu, G.; Wallart, W.; Caroff, P. *Nanotechnology* **2011**, *22*, 275602.
- (29) Ramdani, M. R.; Harmand, J. C.; Glas, F.; Patriarche, G.; Travers, L. *Cryst. Growth Des.* **2013**, *13*, 91–96.
- (30) Glas, F.; Ramdani, M. R.; Patriarche, G.; Harmand, J. C. *Phys. Rev. B: Condens. Matter Mater. Phys.* **2013**, *88*, 195304.
- (31) Glas, F. *Phys. Status Solidi B* **2010**, *247*, 254–258.
- (32) Dubrovskii, V. G.; Sibirev, N. V.; Cirlin, G. E.; Soshnikov, I. P.; Chen, W. H.; Larde, R.; Cadet, E.; Pareige, P.; Xu, T.; Grandidier, B.; Nys, J.-P.; Stievenard, D.; Moewe, M.; Chuang, L. C.; Chang-Hasnain, C. *Phys. Rev. B: Condens. Matter Mater. Phys.* **2009**, *79*, 205316.
- (33) Dubrovskii, V. G.; Xu, T.; Lambert, Y.; Nys, J.-P.; Grandidier, B.; Stievenard, D.; Chen, W.; Pareige, P. *Phys. Rev. Lett.* **2012**, *108*, 105501.
- (34) Hoather, W. H. *Proceedings of the Physical Society* **1936**, *48*, 699–707.
- (35) Dubrovskii, V. G. *J. Chem. Phys.* **2009**, *131*, 164514.
- (36) Dubrovskii, V. G.; Nazarenko, M. V. *J. Chem. Phys.* **2010**, *132*, 114507.
- (37) Dubrovskii, V. G.; Consonni, V.; Geelhaar, L.; Trampert, A.; Riechert, H. *Appl. Phys. Lett.* **2012**, *100*, 153101.
- (38) Sibirev, N. V.; Tchernycheva, M.; Timofeeva, M. A.; Harmand, J. C.; Cirlin, G. E.; Dubrovskii, V. G. *J. Appl. Phys.* **2012**, *111*, 104317.
- (39) Wu, Z. H.; Mei, X. Y.; Kim, D.; Blumin, M.; Ruda, H. E. *Appl. Phys. Lett.* **2002**, *81*, 5177–5179.
- (40) Sabelfeld, K. K.; Kaganer, V. M.; Limbach, F.; Dogan, P.; Brandt, O.; Geelhaar, L.; Riechert, H. *Appl. Phys. Lett.* **2013**, *103*, 133105.
- (41) Fernández-Garrido, S.; Kaganer, V. M.; Sabelfeld, K. K.; Gotschke, T.; Grandal, J.; Calleja, E.; Geelhaar, L.; Brandt, O. *Nano Lett.* **2013**, *13*, 3274–3280.